ANALYSIS OF HEAT TRANSFER IN A TURBULENT PIPE FLOW USING EXTENDED PROPER ORTHOGONAL DECOMPOSITION

Rasmus Korslund Schlander[1*], Stelios Rigopoulos[2], George Papadakis[1]

[1]Department of Aeronautics, Imperial College London, London SW7 2AZ, UK
[2]Department of Mechanical Engineering, Imperial College London, London SW7 2AZ, UK

1. ABSTRACT

A method is presented for investigating the role of coherent structures in turbulent flows on the time-average wall heat transfer by using extended proper orthogonal decomposition (EPOD). The data used for the analysis is from a direct numerical simulation (DNS) of a pipe flow with a Reynolds number of 5300 based on bulk velocity. A Fukagata Iwamoto Kasagi (FIK) identity equation is used to relate the fluctuating velocity and temperature fields to the time-average Nusselt number (Nu). The results show that the temperature-velocity correlations account for up to 65.8% of Nu depending on downstream location. By applying the FIK identity on the POD/EPOD modes, which due to homogeneity are Fourier modes in the azimuthal direction, it is now possible to compute the individual contribution of the coherent structures to the wall heat transfer. By applying the method on the DNS data set, it can be shown that the first 15 wavenumbers and 10 POD modes can reconstruct 50% of the wall heat transfer using velocity modes while containing only 30% of the turbulent kinetic energy.

2. INTRODUCTION

Near wall turbulent coherent structures play an important role in wall heat transfer and have been extensively studied in the past with both simulations and experiments. In H. Nakamura et al. [1], the temperature was measured on the walls of a turbulent pipe flow and long streamwise structures were observed and related to the coherent velocity structures. In Antoranz et al. [2], the fluctuating velocity and temperature field were analysed in a cylindrical solar receiver using POD and EPOD and similar structures were found inside the pipe. Recently, Mallor et. al. [3], used POD to find coherent structures in the wall heat transfer measurements on a flat plate, however, as noted by the authors, only the fluctuating part of the heat transfer was analysed, since POD only analyses fluctuating quantities. This paper therefore presents a method for connecting the fluctuating quantities to the mean values by combining EPOD analysis and the FIK identity. This makes it possible to analyse the contribution of individual near wall turbulent coherent structures to the time-average wall heat transfer.

3. METHODOLOGY

Due to homogeneity, the fluctuating velocity and temperature fields are first decomposed in the azimuthal direction using a Fast Fourier Transform, $q'(r,\theta,z,t) = \sum_m \hat{q}_m(r,z,t)\mathrm{e}^{\mathrm{i}m\theta}$, where m is the azimuthal wavenumber. The eigenvalue problem of POD then becomes, L. Sirovich [4]:

$$\hat{Q}_m^* W \hat{Q}_m \Psi_m = \Lambda_m \Psi_m \qquad \Phi_m = \hat{Q}_m \Psi_m \Lambda_m^{-1/2} \qquad \hat{Q}_m = \Phi_m \Lambda_m^{1/2} \Psi_m^* \qquad (1)$$

$\hat{Q}_m$ is a snapshot matrix containing the Fourier transformed variable, W is a spatial weight, Λ_m is a diagonal matrix containing the eigenvalues, Ψ_m is the matrix containing the temporal coefficient and Φ_m is a matrix containing the spatial modes. The idea behind EPOD is to use the temporal coefficients of one variable such as the temperature, $\Psi_{m,T}$, to reconstruct another variable such as the velocity field, $\Phi_{m,V}^e = \hat{Q}_{m,V} \Psi_{m,T} \Lambda_{m,T}^{-1/2}$, see J. Borée [5] for details. $\Phi_{m,V}^e$ is now the spatial velocity EPOD mode correlated to the temperature field. In order to relate the fluctuating quantities from the POD and EPOD to the total wall transfer on the pipe walls, a FIK identity has been derived by non-dimensionalizing and integrating the convection-diffusion equation twice in the radial direction, Kasagi et al [6]:

*Corresponding Author: r.schlander19@imperial.ac.uk

$$Nu = -\underbrace{\frac{8}{(T_b - T_w)}\int_0^1 \frac{\partial \overline{T}}{\partial r} r\mathrm{d}r}_{Nu_{FIK1}} + \underbrace{\frac{8RePr}{(T_b - T_w)}\int_0^1 r\,\overline{u_r'T'}r\mathrm{d}r}_{Nu_{FIK2}} + \underbrace{\frac{4RePr}{(T_b - T_w)}\int_0^1 (1-r^2)\langle\frac{\partial \overline{u_z}\overline{T}}{\partial z}\rangle r\mathrm{d}r}_{Nu_{FIK3}}$$

$$+\underbrace{\frac{4RePr}{(T_b - T_w)}\int_0^1 (1-r^2)\langle\frac{\partial \overline{u_z'T'}}{\partial z}\rangle r\mathrm{d}r}_{Nu_{FIK4}} - \underbrace{\frac{4}{(T_b - T_w)}\int_0^1 (1-r^2)\langle\frac{\partial^2\overline{T}}{\partial z^2}\rangle r\mathrm{d}r}_{Nu_{FIK5}} \qquad (2)$$

where $\langle\,\rangle$ indicates the operation $\langle f\rangle = \overline{f} - 2\int_0^r f\,r\mathrm{d}r$, the subscript b indicates bulk values, the subscript w indicates wall values.

4. RESULTS

The database used for the analysis is a DNS of a fully developed turbulent pipe flow with a Reynolds number of $Re_B = 5300$ based on streamwise bulk velocity U_B and where the temperature is treated as a passive scalar with a Prandtl number of $Pr = 1$. The grid used for the simulation is unstructured and comprises both O- and H-type meshes with a total of $N_c = 8.6 \cdot 10^6$ cells, with $\Delta r_{min}^+ = 0.4$, $\Delta r_{max}^+ = 7.16$, $R\Delta\theta_{max}^+ = 11.7$, $\Delta z^+ = 10.6$ in wall units. Comparison of the radial profiles of the mean velocity, root mean square (RMS) velocity and Reynolds stresses with reference data from literature are shown in figure 1 and excellent agreement is found.
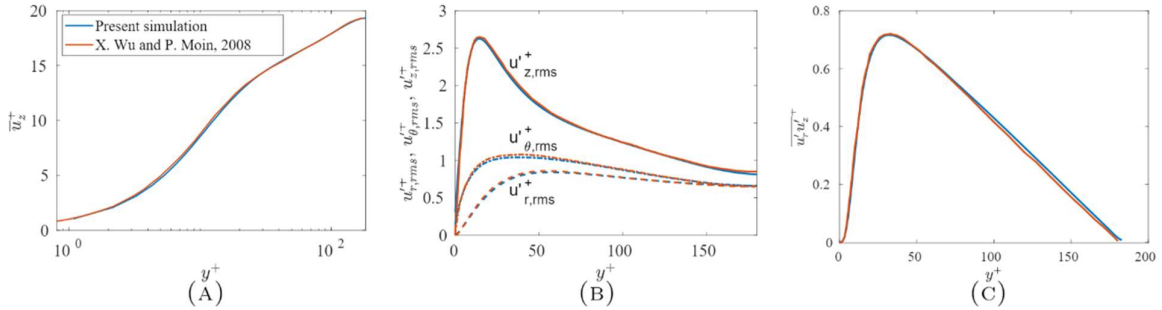
Figure 1: Mean velocity (A), RMS values (B) and shear Reynolds stresses (C) are compared to X. Wu. And P. Moin [7].

The POD and EPOD analysis is based on 600 snapshots of the flow and temperature field interpolated in a structured grid (r, θ, z) with $(N_r, N_\theta, N_z) = (256,128,256)$ data points, each separated in time with $\Delta t = 0.95R/U_B$. The eigenvalues from the decomposition are plotted in figure 2, and a peak is observed for wavenumber m=6 for the temperature and m=4 for the velocity correlated with the temperature.
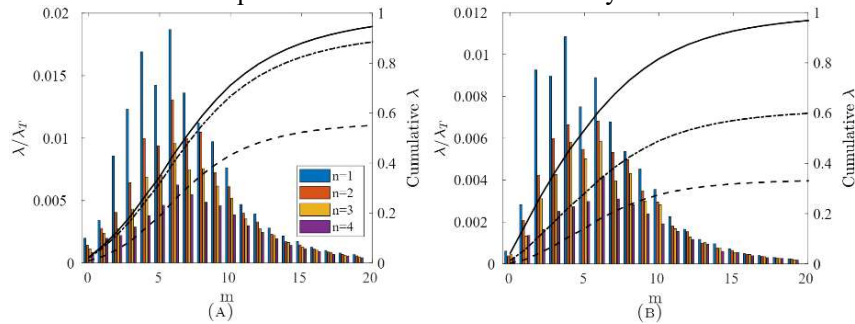
Figure 2: Distribution of the eigenvalues of the temperature POD modes normalized with temperature variance (A) and distribution of the turbulent kinetic energy of the velocity EPOD modes normalized with total turbulent kinetic energy (B). Left vertical axis shows the relative energy of each mode, and right shows the cumulative energy along wavenumbers, where (--) is n=1-15, (-.-) is n=1-100 and (-) is n=1-200. Modes n=1-4 are also plotted for individual azimuthal wavenumbers.

The spatial distribution of mode n=1 with azimuthal wavenumber m=2,4,6 is plotted in figure 3. It is observed that both POD and EPOD modes have a smaller presence near the centre with increasing wavenumber. The components of equation 2 are plotted in figure 4A, and at 7.5D, 65.8% of the wall heat transfer can be attributed to Nu_{FI} i.e., to temperature-velocity correlations. Note the excellent matching between the Nu predicted by DNS and by summing the different components of equation 2.

In order to quantify the contributions of the POD and EPOD modes to the wall transfer, Nu_{FIK2} is calculated for individual modes and is integrated along the streamwise axis $\Gamma_{m,n} = \int_0^{7.5D} Nu_{FIK2}(m,n)\mathrm{d}z$. The wall heat transfer related to each POD and EPOD is plotted in figure 4B.
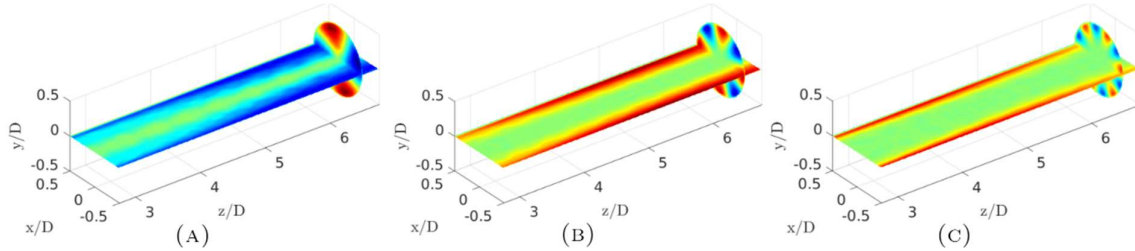
Figure 3: Dual-plane contour plot of the first velocity EPOD mode using $m = 2$ (A), $m = 4$ (B) and $m = 6$ (C), where red and blue represent positive and negative values, respectively.

By applying this method, it can be shown that the POD/EPOD mode pair m=6, n=1 has the largest contribution to the wall heat transfer. By combining the first 15 azimuthal wavenumbers and 10 POD numbers it is possible to reconstruct 50% of the wall heat transfer, despite the modes only containing 30% of the turbulent kinetic energy, and by combining m=1-20 and n=1-100, it is possible to reconstruct 90% of the wall heat transfer using velocity modes containing 57% of the kinetic energy.
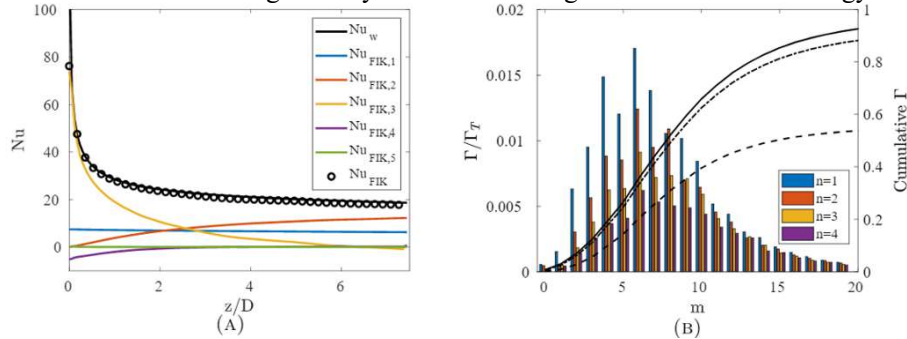
Figure 4: Contributions of different components to the Nusselt number using equation 2 (A). Individual contributions of wavenumbers, m, and POD numbers, n, to the wall transfer Γ (B). Left vertical axis shows the wall transfer of each mode, and right shows cumulative the wall transfer along wavenumbers, where (--) is n=1-15, (-.-) is n=1-100 and (-) is n=1-200 . Modes n=1-4 are also plotted for individual azimuthal wavenumbers.

To provide further insight, we now analyse the contribution of each mode in relation to its kinetic energy; which is plotted in figure 5(A) for single wavenumbers and 5(B) for groups of wavenumbers. Intuitively, the larger the energy of a mode, the more it will contribute to the total wall heat transfer, so we expect a positive correlation. The steeper the slope, the larger the contribution of a mode for a given turbulent kinetic energy or temperature variance. As can be seen from figure 5(A), there is a large spread in the slopes of the velocity EPOD modes (solid lines), but the spread is much smaller for the slope of temperature modes (dashed lines). Interestingly, while velocity EPOD modes with $m = 6$ may have the largest overall contribution to the wall transfer in absolute terms (solid yellow line in Fig. 5(A), modes with $m = 8$ have a slightly larger slope and are thus more efficient. Figure 5(B) shows that increasing the range of m values, the cumulative transfer reaches an asymptotic relation with respect to the kinetic energy contained within the EPOD modes. This slope is larger compared to the one relating the transfer and the variance of temperature modes.
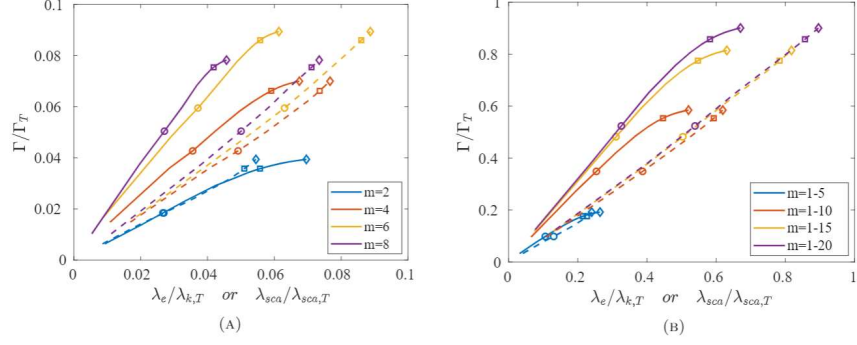
Figure 5: Γ/Γ_T plotted against eigenvalues for single wavenumbers (A) and groups of wavenumbers (B). In both figures, solid lines represent eigenvalues from velocity EPOD modes, and dashed lines eigenvalues from temperature POD modes. A circle corresponds to $n = 1 - 10$, a square to $n = 1 - 100$ and a diamond to $n = 1 - 200$.

5. CONCLUSIONS

The presented method makes it possible to analyse coherent structures and link these to the time-average wall heat transfer, and to find modes that contribute disproportionally to the wall heat transfer compared to their turbulent kinetic energy.

Future work will explore the potential of the methodology for gaining insight into more complex settings that may include chemical reactions and different flow configurations. This approach can also be exploited to actively or passively control the wall heat transfer rate, in the same way that the understanding of the effect of different flow structures in the skin friction have recently led to the developments of drag reducing actuation strategies that offer net power savings, even in large Re numbers.

REFERENCES

[1]   H. Nakamura, N. Shiibara, and S. Yamada, Quantitative measurement of spatio-temporal heat transfer to a turbulent water pipe flow. *International Journal of Heat and Fluid Flow*, (2017) 63:46–55

[2]   A. Antoranz, A. Ianiro, O. Flores, and M. García-Villalba, Extended proper orthogonal decomposition of non-homogeneous thermal fields in a turbulent pipeflow. *I. J. of Heat and Mass Transfer*, (2018) 118:1264–1275.

[3]   F. Mallor, M. Raiola, C. Sanmiguel Vila, R. Örlü, S. Discetti, and A. Ianiro, Modal decomposition of flow fields and convective heat transfer maps: An application to wall-proximity square ribs, *Exp. Therm. Fluid Sci.*, (2019) vol 102, pp. 517–527

[4]   L. Sirovich, Turbulence and the dynamics of coherent structures part I: coherent structures, *Quarterly of Applied Mathematics*, (1987). 45(3):561–571

[5]   J. Borée, Extended proper orthogonal decomposition: a tool to analyse correlated events in turbulent flows, *Exp. Fluids*, (2003) vol. 35, no. 2, pp. 188–192,

[6]   N. Kasagi, Y. Hasegawa, K. Fukagata, and K. Iwamoto, Control of Turbulent Transport: Less Friction and More Heat Transfer, *J. Heat Transfer*, (2012) vol. 134, no. 3

[7]   X. Wu. And P. Moin, A direct numerical simulation study on the mean velocity characteristics in turbulent pipe flow, *Journal of Fluid Mechanics,* (2008) 608:81–112,